Assessing the impacts of climate variability and human activities on annual runoff in the Luan River basin, China

Xiangyu Xu, Hanbo Yang, Dawen Yang and Huan Ma

ABSTRACT

Regional hydrological processes have been greatly influenced by human activities and climate variability. The inflow of Panjiakou Reservoir, which is the largest reservoir located on the Luan River, has shown a significant decreasing trend over the past 50 years. A large-scale hydrological model, namely the geomorphology-based hydrological model (GBHM), and a climate elasticity model were applied to perform quantitative attributing analysis of runoff change in the study catchment. Annual runoff decreased by 19.5 mm from 65.7 mm in the period 1956–1979 to 46.2 mm in the period 1980–2005. Annual direct water intake increased by 22.5 mm from 3.6 to 26.1 mm. Climate impact was accountable for the runoff increase of 8.8 and 9.2 mm simulated by GBHM and the climate elasticity model, respectively. Impacts of land use and vegetation change accounted for the runoff decrease of 2.5 mm. Change of precipitation and vegetation cover contributed to annual runoff change for the upper catchment (grassland-dominated). Change of antecedent precipitation (a proxy of soil moisture) also contributed to annual runoff change for the lower catchment (forest-dominated) and the whole catchment (mixture vegetation).

Key words | climate variability, human activity, hydrological model, Luan River basin, runoff decrease

Xiangyu Xu
Hanbo Yang
Dawen Yang (corresponding author)
Huan Ma
State Key Laboratory of Hydro-Science and Engineering,
Department of Hydraulic Engineering,
Tsinghua University,
Beijing, 10084,
China
E-mail: *yangdw@tsinghua.edu.cn*

Huan Ma
The Haihe River Water Conservancy Commission of the Ministry of Water Resources,
Tianjin, 300170,
China

INTRODUCTION

The watershed hydrological processes have been greatly influenced by climate variability (NRC 1991; IPCC 2007) and human activities (Scanlon *et al.* 2007; Barnett *et al.* 2008). Changes in runoff have been observed worldwide. Runoff of most catchments in the United States has been increasing since at least 1940 (Lins & Slack 1999; McCabe & Wolock 2002). However, most rivers in northern Canada have experienced decreasing runoff (Déry & Wood 2005; McClelland *et al.* 2006). Runoff in the Amazon River has shown a decreasing trend during the last 20 years (Costa & Foley 1999). Most northern European rivers also showed little change, whereas many circum-Mediterranean rivers declined considerably (Milliman *et al.* 2008). Significant increase in runoff was observed in the Blue Nile River during the period 1964–2003 (Tesemma *et al.* 2010). Most river basins in north China, such as the Hai River (Ren 2007; Ma *et al.* 2010), the Yellow River (Yang *et al.* 2004; Li *et al.* 2007; Wang *et al.* 2008; Cong *et al.* 2009) and the Shiyang River (Ma *et al.* 2008) have shown a significant decreasing trend in annual runoff in the last 50 years.

In recent years, many studies have attempted to quantify the effects of climate variability and human activities on the change in catchment runoff. Qian *et al.* (2007) reported that annual runoff increased in the Mississippi River basin from 1948 to 2004, and according to Twine *et al.* (2004), this change could mainly be attributed to precipitation increase and land cover change. Xu *et al.* (2008) analyzed the spatial and temporal variations in runoff in the Yangtze River over the last 40 years using qualitative analysis, and the decreasing trend can be attributed to climate variability and human activities, including reservoir construction and water consumption. Piao *et al.* (2007) found that land use change was the second most important driver in the decrease in global runoff from 1901 to 1999 followed by climate variability. Gerten *et al.* (2008) used a global vegetation and

doi: 10.2166/nh.2013.144

hydrology model to quantify the contributions of different drivers to worldwide trends of runoff in the 20th century, and they found that changing precipitation was the most important factor, followed by land use change, rising atmospheric CO_2 content, global warming, and irrigation.

Two main approaches are widely used for the quantitative assessment of changes in runoff. One is the statistical regression analysis and the other is hydrological modeling. Statistical regression analysis is usually used for estimating the impacts of climate variability on annual runoff. Revelle & Waggoner (1983) used multivariate statistical analysis to estimate the relationship between the changes in climate and runoff in the western United States. Vogel *et al.* (1999) used a regional multivariate regression model and showed that a 10% increase in precipitation would lead to a 19% increase in annual runoff in the entire upper Colorado River. Schaake (1990) proposed a simple climate elasticity model to evaluate the effects of climate variability on annual runoff based on the observed precipitation and runoff data. Sankarasubramanian *et al.* (2001) analytically derived runoff elasticity to precipitation change using the Turc-Pike equation based on the Budyko hypothesis. The latter includes a conceptual water balance model (Budyko 1974; Fu 1981; Roderick & Farquhar 2011; Yang & Yang 2011) and the distributed hydrological model, which were successfully employed to attribute the runoff change to the impacts of climate variability and land use/cover change. Onstad & Jamieson (1970) first used a hydrological model to predict the runoff change caused by land use change. Simulations showed that replacing forest, woodland, and savanna with grassland over the Amazon River basin (Costa & Foley 1997) and deforestation in the Columbia River basin, either through species replacement or logging (Matheussen *et al.* 2000) would increase runoff. Runoff trends have been quantitatively analyzed to evaluate the impacts of climate variability and human activities in the Yellow River using a large-scale hydrological model, namely, the geomorphology-based hydrological model (GBHM) (Cong *et al.* 2009). Ma *et al.* (2010) also used the GBHM to quantify the contributions of climate variability in the decrease in inflow into the Miyun Reservoir, which is the major surface water resource of Beijing.

The Luan River basin is a sub-basin of the Hai River in northern China. The Panjiakou Reservoir, constructed in 1982 on the middle reach of the Luan River, was planned to be a major water resource for Tianjin and Tangshan cities located downstream. However, runoff in the upstream of the Panjiakou Reservoir significantly decreased after its construction resulting in a severe water shortage in the downstream region. Thus, knowing the reasons for the decrease in runoff and how much the impacts of climate variability and human activities contribute to this change are desirable to improve the water resources management in the Luan River basin and predict future change in runoff.

The current study primarily aims to estimate the impacts of human activities and climate variability on the decrease in annual runoff in the Luan River basin. First, the trend of annual runoff, annual precipitation, and annual air temperature from 1956 to 2005 were detected. Second, the cause of the annual runoff change was determined by the GBHM and the climate elasticity model.

STUDY AREA AND DATA

The Luan River flows from the northwest to the southeast and discharges directly into the Bohai Sea, which is part of the Hai River basin. The upper reach of the Luan River basin is located in Inner Mongolia, with grasslands as its major vegetation type. The middle and lower reaches of the Luan River basin are mainly located in Hebei province with major vegetation of forests. The whole Luan River basin has an average annual precipitation of 455 mm, with approximately 75–85% of the annual total concentrates during the flood season (from June to September). The Panjiakou Reservoir has a total storage capacity of 2.9 billion m^3, and is the largest reservoir located on the Luan River. The upstream watershed of the Panjiakou Dam was selected as the study area, as shown in Figure 1. The drainage area is about 33,700 km^2, occupying nearly 75% of the Luan River basin. The catchment is located in the region delimited by geographical coordinates 40.4° to 42.6° N and 115.5° to 118.9° E with the elevation ranging from 144 to 2,228 m (see Figure 1).

The topography of the catchment was represented using the digital elevation model (DEM) with 90 m resolution from the global topography database (http://telascience.sdsc.edu/tela_data/SRTM/version2/SRTM3/). Digital land-use maps with 100 m resolution in the 1980s and 1990s were obtained from the Data Center for Resources and Environmental

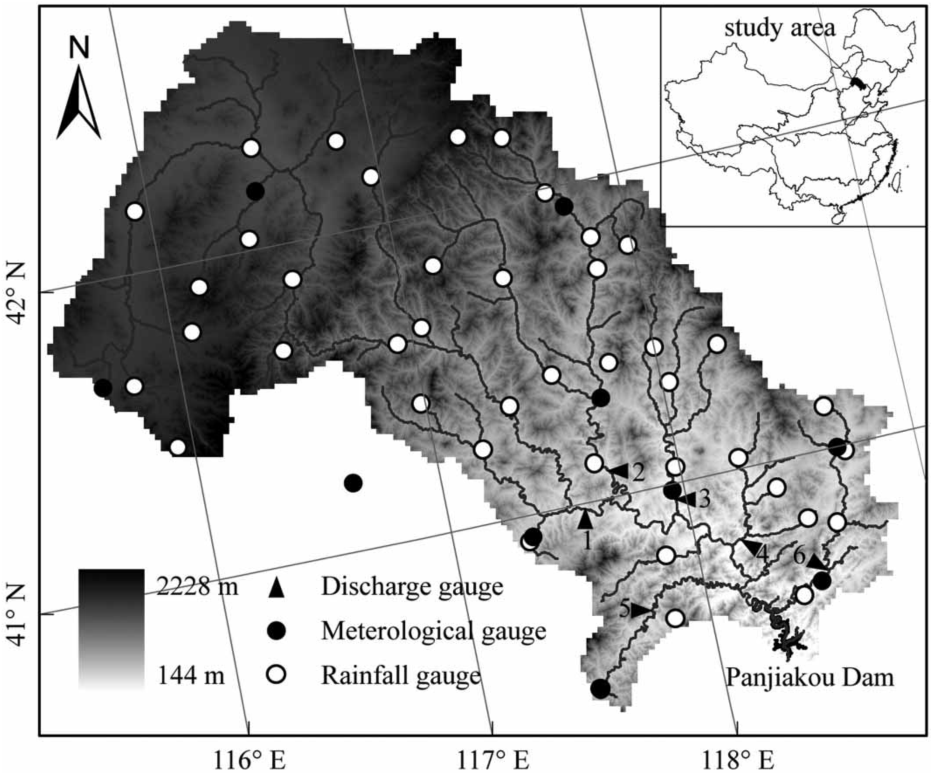

Figure 1 | Location of the study area in China and locations of discharge gauges, meteorological gauges and precipitation gauges (discharge gauges 1–6 are the Sandaohezi, Hanjiaying, Chengde, Xiabancheng, Liying, and Kuancheng, respectively).

Sciences in the Chinese Academy of Sciences. In the GBHM, the primary land-use types were resampled into nine types including water body, urban area, forest, irrigated cropland, non-irrigated cropland, grassland, shrub, bare soil, and wetland. The soil type used in this study was based on the Food and Agriculture Organization (FAO)-UNESCO classification and the Soil Map of the World at a spatial scale of 1:5 million was obtained from the FAO. Six different soil types existed in the study catchment. The top-soil depth with a 1:1 million-scale resolution was obtained from the soil database of China. The seasonal changes in vegetation were expressed using the monthly leave area index (LAI), which was estimated from the monthly normalized difference vegetation index (NDVI) from the Data and Information Services Center (DAAC) website of GSFC/NASA (http://daac.gsfc.nasa.gov/DAAC_DOCS/) with an 8 km resolution from 1981 to 2006.

Meteorological data, including precipitation, maximum, minimum, and mean air temperature, wind speed, relative humidity, and sunshine hours, were obtained from the China Meteorological Administration. Additional daily precipitation data were obtained from the Hydrological Year Book. There are 10 meteorological stations and 41 rainfall gauges in/nearby the study catchment and all stations have continuous records from 1956 to 2005. Daily inflow into the Panjiakou Reservoir and the daily runoff at eight upstream hydrological stations were obtained from the Hydrological Year Book published by the Hydrological Bureau of the Ministry of Water Resources. The monthly statistical data of direct water intake from 1956 to 2000 were collected during the Second National Water Resources Assessment Project (Ren 2007). The direct water intake included water consumption in the agriculture sector, industry, and domestic use in the upstream of the Panjiakou Dam.

METHODOLOGY

Changes in runoff could be attributed to the impact of climate variability and human activities, such as land-use change and direct water intake. In addition, climate variability and human activities could affect vegetation cover. Changes in runoff might be related to change in vegetation cover because of the interactions between hydrological processes and vegetation dynamics. Figure 2 shows the framework of correlations between climate, runoff, and vegetation. The solid arrows depict the relative strong and direct effects that have been estimated and the dashed arrows depict indirect effects that have not been considered in this study. In this study, climate variability primarily refers to the variations in precipitation and air temperature. The impact of climate variability was estimated using both the GBHM and the climate elasticity model, and both models offered an inter-comparison for the assessment. The impacts of human activities on runoff include direct water intake and indirect impact of land use and vegetation changes. Direct water intake was calculated from monthly statistical data (Ren 2007), and the indirect impact of changes in land use and vegetation cover were simulated using the GBHM. The trend analysis was applied to the time series of annual runoff, annual precipitation, and annual air temperature prior to quantitative assessments.

Trend analysis

The Mann–Kendall (MK) nonparametric test (Kendall & Gibbons 1990) has been recommended as an effective tool for trend detection (Maidment 1992). In the current study, the MK test was used to determine the significance of the trends in annual meteorological and hydrological time series. The significance levels of the trend test were set at 5% and 10%. The slope of the trend was estimated as follows (Burn & Elnur 2002):

$$\beta = \text{median}\left[\frac{(x_j - x_i)}{(j - i)}\right] \quad (1)$$

for all $i < j$, where β is the trend magnitude. A positive value of β indicates an increasing trend, and a negative value of β indicates a decreasing trend.

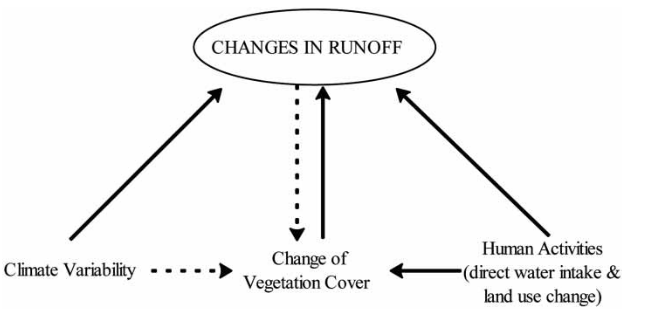

Figure 2 | Impacts of climate variability and human activities on runoff change. (*Note:* The solid arrows indicate the relative strong and direct effects that have been estimated in this study, whereas the dashed arrows indicate indirect effects that have not been considered in this study.)

Climate elasticity model

The climate elasticity model (Schaake 1990; Sankarasubramanian *et al.* 2001; Ma *et al.* 2010) is usually used for assessing the climate variability impact on runoff change. Most previous studies did not consider the influence of soil moisture change. Xu *et al.* (2012) used the antecedent precipitation as a proxy of soil moisture and the soil moisture storage is taken as a function of the antecedent precipitation, which could be expressed as:

$$S = f(P_{-1}, P_{-2}, P_{-3}, \cdots) \quad (2)$$

where P_{-1}, P_{-2}, P_{-3} are the annual precipitation in previous years.

The revised climate elasticity model can be expressed as follows:

$$\frac{\Delta R_i}{\overline{R}} = \varepsilon_R^P \frac{\Delta P_i}{\overline{P}} + \varepsilon_R^{P_{-1}} \frac{\Delta P_{-1}}{\overline{P}} + \cdots + \varepsilon_R^{P_{-n}} \frac{\Delta P_{-n}}{\overline{P}} + \varepsilon_R^T \Delta T_i \quad (3)$$

where $\Delta R_i/\overline{R} = (R_i - \overline{R})/\overline{R}$ and $\Delta P_i/\overline{P} = (P_i - \overline{P})/\overline{P}$ represent the annual percentage departures from mean annual values for runoff and precipitation, respectively, ΔT_i represents the change in annual mean temperature compared to the long-term mean temperature ($\Delta T_i = T_i - \overline{T}$), $\varepsilon_R^{P_{-1}}, \ldots, \varepsilon_R^{P_{-n}}$, represents the runoff elasticity to soil moisture change, meaning the percent change of runoff coming from the change of precipitation in previous years, and ε_R^T is the runoff elasticity to temperature change, meaning the percent change in runoff coming from the change of temperature by 1 °C.

Based on Equation (3), the elasticities could be estimated by regression analysis step by step using the data in the calibration period. The R^2 statistic, the t statistic and its p value, and an estimate of the error variance are calculated to determine how many terms should be considered in Equation (3). The annual runoff departure from mean annual runoff could then be estimated by Equation (3). The annual runoff could be calculated by:

$$R_i = \Delta R_i + \overline{R} \tag{4}$$

The mean annual runoff could be averaged by the annual runoff in the prediction period. The difference of mean annual runoff between two periods could be considered as the impacts of climate variability on runoff.

Large-scale distributed hydrological model

The GBHM, which is a large-scale hydrological model, was used to simulate the hydrological processes in the study area. The GBHM was developed by Yang *et al.* (1998, 2002) and has been successfully applied in the Yellow River (Cong *et al.* 2009), the Yangtze River (Xu *et al.* 2008), and the Panjiakou Reservoir catchment (Xu & Yang 2009).

The pre-preparation procedures contain catchment subdivision and sub-grid parameterization. The Panjiakou Reservoir catchment was divided into 97 sub-catchments by the Pfafstetter scheme (Yang & Musiake 2003) to effectively represent the topography, and the GBHM was employed in each sub-catchment. A simplified stream network is composed of the main streams of all subcatchments. All hillslopes are assumed to contribute to the same main stream. Therefore, the two-dimensional catchment is simplified into a one-dimensional cascade of flow intervals linked by the main stream, and each flow interval comprises a set of parallel hillslopes. The hillslope is the fundamental unit of computation in the hydrological model, which provides the lateral inflow to the main stream. The catchment runoff is the integration of hillslope responses through the river routing.

The geomorphologic property of stream–hillslope formation was used to represent catchment topography and a large grid was assumed to be composed of a set of hillslopes located along the streams. The runoff generated from one grid is the sum of the hillslope responses including both surface and subsurface runoffs. The vertical flux, which is the actual evapotranspiration, is the total evapotranspiration simulated from all the hillslopes. The soil moisture content state variable is taken as the area-averaged soil moisture of all the hillslopes.

The parameters used in the model included vegetation parameters, land surface parameters, soil–water properties, river parameters, a snow-melting parameter, and a groundwater parameter. Since most of the parameters have physical meanings, they can be estimated through field tests. However, measuring all parameters for such a large basin is impossible. Therefore, this study specified the model parameters by referring to existing databases and handbooks. The snowmelt factor in the temperature-based snowmelt equation was one of the calibrated parameters in this model. The hydraulic conductivity of the groundwater, which was calibrated by checking the baseflow using a baseflow separation technique in different subbasins, was another calibrated parameter.

The impact of climate variability on annual runoff change was assessed using the GBHM using the same scenario of land use/cover condition for period 1 (1956–1979) and period 2 (1980–2005). The 1980s land-use map (LU1) was used to represent the original condition with relatively few human activities. The difference of mean annual runoff between period 1 and period 2 under LU1 was considered as the impact of climate variability on runoff. The indirect impact of human activities (land use/cover change) on annual runoff change was also assessed using the GBHM. The GBHM was conducted using the same scenario of climate conditions as observed from 1980 to 2005 and the changing conditions in land use/cover. The 1990s land-use map (LU2) was used to represent the scenario of land use change. The difference of the mean annual runoff in period 2 between LU2 and LU1 was considered as the indirect impact of human activity on runoff.

RESULTS

Observed changes in climate variables and runoff

The trends and its significances of the annual runoff, precipitation, and air temperature were first detected using the MK test. Inflow into the Panjiakou Reservoir from 1956 to 2005 depicted a decreasing trend of 0.31×10^8 m^3/a (0.91 mm/a) at the 5% significance level, as shown in Figure 3(a). The annual air temperature increased by 0.023 °C/a at the 5% significance level, as shown in Figure 3(b). The annual precipitation of the study catchment showed a non-significant ($p = 0.42$) increasing trend of 0.54 mm/a, as shown in Figure 3(c). The flood season precipitation (precipitation from June to September) showed a non-significant ($p = 0.15$) increasing trend of 1.14 mm/a, as shown in Figure 3(d). From Figures 3(c) and 3(d), we can see that the increase in annual precipitation comes from an increase in summer precipitation, which has a more significant trend. Therefore, winter precipitation, which may fall as snow, decreased from 1956 to 2005.

The upstream catchment of the Sandaohezi gauge (discharge gauge 1 in Figure 1), which is termed the 'upper catchment', the catchment between the Sandaohezi gauge and Panjiakou Dam, called the 'lower catchment', and the whole Panjiakou catchment were investigated to distinguish differences in runoff changes and their dominant drivers. The long-term average and trend of annual precipitation, air temperature, runoff, and direct water intake are summarized in Table 1. The upper and lower catchments had a similar drainage area, but the upper catchment was grassland dominated by colder and drier climates (mean daily temperature of 2.8 °C and mean annual precipitation of 401.4 mm), whereas the lower catchment was forest dominated with relatively warm and wet climates (mean daily temperature of 4.8 °C and mean annual precipitation of 519.3 mm). The annual runoff in the upper catchment from 1956 to 2005 depicted a decreasing trend of 1.62 mm/a at the 10% significance level, but the annual runoff in the lower catchment showed a non-significant ($p = 0.63$) decreasing trend.

Figure 4 shows the observed annual inflow into the Panjiakou Reservoir and the annual statistical value of the direct water intake from the upper region of the dam. It is clear that the direct water intake had significantly increased since 1980. The inflow into the Panjiakou Reservoir was much larger from 1956 to 1979 than from 1980 to 2005, with especially a steep decrease occurring in 1980, which also could be seen from the series of runoff coefficient shown in Figure 3(a). For simplification, the study period was split into two sub-periods (period 1: 1956–1979 and period 2: 1980–2005). As shown in Table 2, the observed runoff of the study catchment was 65.7 mm in period 1 and 46.2 mm in period 2. The annual precipitation and mean daily temperature in the study catchment were 430.2 mm and 3.5 °C in period 1, and were 458.7 mm and 4.0 °C in period 2, respectively.

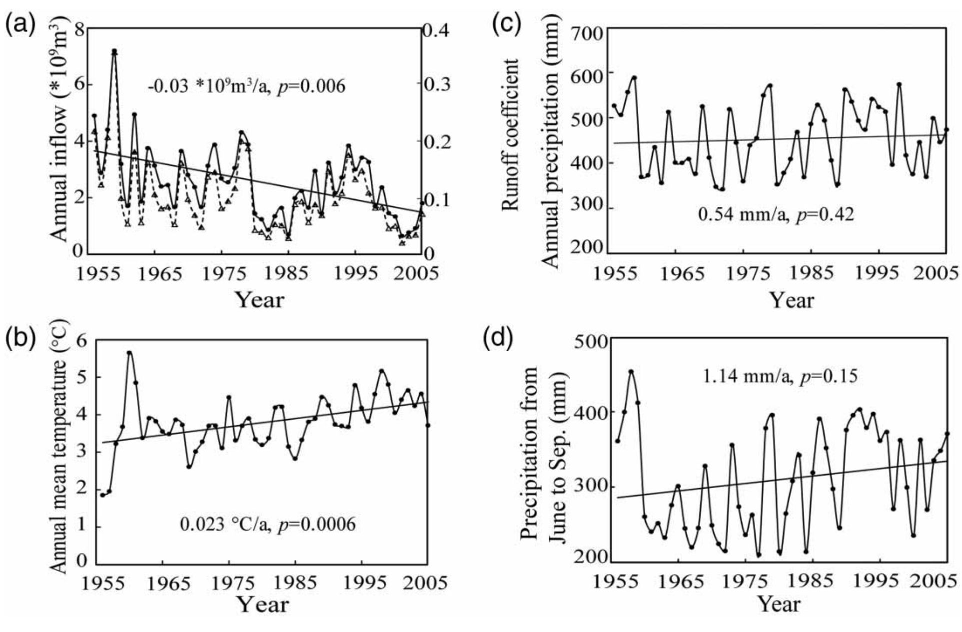

Figure 3 | Trend analyses of annual runoff, temperature, and precipitation of the Panjiakou Reservoir catchment. (a) Observed annual inflow (10^9 m^3) into the Panjiakou Reservoir (solid line) and annual runoff coefficient (dashed line); (b) annual air temperature (°C); (c) annual precipitation (mm); (d) precipitation (mm) from June to September.

Table 1 | Statistics of the climate variables, runoff, direct water intake, and vegetation in the upper, lower, and whole catchments from 1956 to 2005

Region		Upper catchment	Lower catchment	Whole catchment
Area (km^2)		171,00	166,00	337,00
Precipitation	Mean (mm)	401.4	519.3	454.6
	Trend (mm/a)	−1.62	0.68	0.54
	α^a (p value)	10% (0.07)	>10% (0.63)	>10% (0.42)
Temperature	Mean (°C)	2.83	4.79	3.80
	Trend (°C/a)	0.025	0.023	0.023
	α (p value)	5% (0.003)	5% (0.004)	5% (0.0006)
Runoff	Mean (mm)	35.9	95.1	61.0
	Trend (mm/a)	−0.52	−0.91	−0.80
	α (p value)	5% (0.004)	>10% (0.27)	5% (0.006)
Direct water intake (mm)		2.5	25.7	14.1
Major vegetation type		Grassland dominated	Forest dominated	Mixture vegetation
Frost and shrub	LU1 (%)	29.0	48.8	37.6
	LU2 (%)	30.8	56.7	43.5
Grassland	LU1 (%)	41.2	26.6	34.0
	LU2 (%)	39.2	20.8	30.2

[a]α is the significance level.

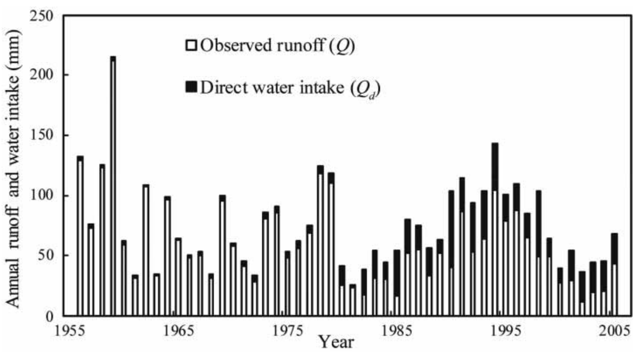

Figure 4 | Comparison of the observed annual runoff with the annual direct water intake in the upstream catchment of the Panjiakou Reservoir from 1956 to 2005.

The changes in observed runoff and climate variables in the upper and lower catchments during the two periods are also shown in Table 2. Both the upper and lower catchments had a common decrease in annual runoff. Annual runoff in the upper catchment decreased by 8.3 mm (23.1%), which is much less than that in the lower catchment which decreased by 34.5 mm (31.4%). The annual precipitation decreased by 9.7% in the upper catchment but increased by 1.8% in the lower catchment.

Model performance

Table 3 shows the statistical results of stepwise regression analysis of the climate elasticity model described in Equation (3). The F statistic in the climate elasticity model considering four consecutive years of precipitation and temperature is 11.756 and its p value is less than 0.001. From Table 3, we can see that annual precipitation (P), air temperature (T), and last year's precipitation (P_{-1}, meaning carry-over of soil moisture storage, which includes the snowmelt from the previous winter) are the three main factors significantly ($p < 0.1$) affecting annual runoff. Therefore, the climate elasticity model described by $\Delta R_i/\overline{R} = \varepsilon_R^P(\Delta P_i/\overline{P}) + \varepsilon_R^{P_{-1}}(\Delta P_{-1}/\overline{P}) + +\varepsilon_R^T \Delta T_i$ was used to estimate the parameters based on the annual runoff, precipitation, and air temperature of the study catchment in period 1. The F statistic of the model is 18.212 and its p value is less than 0.001. In the whole study area, the values of ε_R^P, $\varepsilon_R^{P_{-1}}$ and ε_R^T were obtained as 2.6, 0.5, and −0.07, respectively, indicating that a 1% increase in P, and P_{-1} could cause a 2.6% and 0.5% increase in R, respectively, and a change of +1 °C could cause a 0.07% decrease in R. The climate elasticity model given by

Table 2 | Changes in observed inflow, climate variables, and direct water intake in the upper, lower, and whole catchments

		1956–1979	1980–2005	Change between two periods	
Upper catchment					
Observed river runoff (mm)		40.2	27.8	−8.3	−23.1%
Climate variability	Precipitation (mm)	423.1	381.7	−41.4	−9.7%
	Temperature (°C)	2.6	3.1	0.5	19.2%
Direct water intake (mm)		1.7	3.7	2.0	117.6%
Lower catchment					
Observed river runoff (mm)		109.8	75.3	−34.5	−31.4%
Climate variability	Precipitation (mm)	507.8	517.0	9.3	1.8%
	Temperature (°C)	6.6	7.4	0.8	12.1%
Direct water intake (mm)		8.8	49.5	40.7	462.5%
Whole catchment					
Observed inflow (mm)		65.7	46.2	−19.5	−29.7%
Climate variability	Precipitation (mm)	430.2	458.7	28.5	6.6%
	Temperature (°C)	3.6	4.1	0.5	13.9%
Direct water intake (mm)		3.6	26.1	22.5	625.0%

Table 3 | The statistical results of stepwise regression analysis

	$\Delta P/\overline{P}$	$\Delta P_{-1}/\overline{P_{-1}}$	$\Delta P_{-2}/\overline{P}_{-2}$	$\Delta P_{-3}/\overline{P}_{-3}$	$\Delta T/\overline{T}$
t statistic	6.665	1.808	0.71	1.699	−2.160
p value	<0.001	0.08	0.94	0.10	0.04

$\Delta R_i/\overline{R} = 2.58(\Delta P_i/\overline{P}) + 0.47(\Delta P_{-1}/\overline{P}) - 0.07\Delta T_i$ was used to simulate the changes in annual runoff into the reservoir during period 2.

The direct water intake and flow regulation were not considered in hydrological processes simulated by GBHM. The earlier period (1960–1979) was selected to calibrate and validate the hydrological model because of the relatively small amounts of direct water intake (see Figure 4). The model was calibrated using the historical data from 1960 to 1969 and validated against the observed data during the period 1970–1979. A preliminary numerical experiment was conducted using the observed data from 1960 to 1969 to establish a relatively stable groundwater level and reasonable soil moisture content. Then, the groundwater level and soil moisture content at the end of the test run were adopted and specified as the initial conditions for the long-term simulation run for the period 1956–2005. The Nash–Sutcliffe efficiency (NSE) coefficient (Nash & Sutcliffe 1970) and the relative error (RE) between the monthly simulated and observed runoff were selected as the quantitative evaluation indexes of the simulated hydrographs. The values of NSE were 0.89 and 0.85 and the values of RE were 1.7% and 2.2% for the calibration and validation periods, respectively. In addition, six other gauges (see Figure 1) were used for model validation. All the results showed that the model had sufficient accuracy for long-term simulation of river discharge. Figure 5 shows the simulated and observed discharge into the Panjiakou Reservoir during the calibration and validation periods, respectively. The determinant coefficient of annual runoff estimation by the GBHM for period 1 was nearly 1.00, which is comparative to the value of 0.94 estimated by the climate elasticity model.

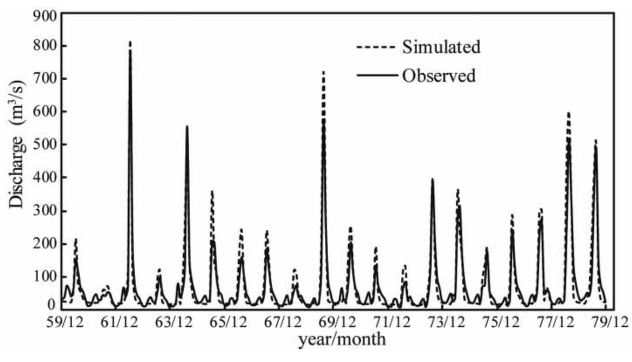

Figure 5 | Observed and simulated monthly inflow into the Panjiakou Reservoir in the calibration and validation periods (calibration period: 1960–1969; validation period: 1970–1979).

Impacts of climate variability on annual runoff

Simulated annual inflow into the Panjiakou Reservoir was 68.1 mm during period 1 and 77.3 mm during period 2 using the climate elasticity model, with an increase of 9.2 mm from period 1 to period 2. Simulated annual runoff in the upper catchment was 38.9 mm during period 1 and 30.4 mm during period 2 with a decrease of 8.5 mm. Simulated annual runoff in the lower catchment was 105.6 mm during period 1 and 116.0 mm during period 2, with an increase of 10.4 mm (see Table 4). Therefore, the impacts of climate variability on runoff were an increase of 9.2 mm, a decrease of 8.5 mm, and an increase of 10.4 mm for the whole, upper, and lower catchments, respectively.

The mean annual runoff of periods 1 and 2 was also calculated based on the GBHM simulation. The difference in the mean annual runoff of the whole study area between the two periods, which was 8.8 mm, from 62.5 to 71.3 mm (Table 4), could be considered as the impact of climate variability. The difference of 8.8 mm is comparatively close to the estimated value of 9.2 mm estimated from the regression method. The impacts of climate variability on runoff were a decrease of 8.4 mm and an increase of 9.7 mm for the upper and lower catchments, respectively.

Impacts of human activity change on annual runoff

Table 2 shows that the annual direct water intake was 3.5 mm in period 1 and 26.1 mm in period 2. Therefore, the direct impact of human activities for the whole catchment was 22.6 mm. The dramatic increase in direct water intake from period 1 to period 2 is due to the increasing demand for water for living, industry, and agriculture with the increase in population, development of economic

Table 4 | Impacts of climate variability and human activities on annual runoff change in the study catchment

		Impact of climate variability		Impact of human activity	
	Observed inflow	Simulated by elasticity model	Simulated by GBHM model	Simulated by GBHM model	Estimated from the water intake
Upper catchment					
1956–1979 (mm)	40.2	38.9	39.2		1.7
1980–2005 (mm)	27.8	30.4	30.8	30.8 (LU1) 29.5 (LU2)	3.7
Change between two periods (mm)	−12.4	−8.5	−8.4	−1.3	+2.0
Contribution to the decrease of river runoff		69.3%	67.7%	10.4%	16.1%
Lower catchment					
1956–1979 (mm)	109.8	105.6	106.1		8.8
1980–2005 (mm)	75.3	116.0	115.8	115.8 (LU1) 112.7 (LU2)	49.5
Change between two periods (mm)	−34.5	+10.4	+9.7	−3.1	+40.7
Contribution to the decrease of river runoff		−30.1%	−28.1%	9.0%	118.0%
Whole catchment					
1956–1979 (mm)	65.7	68.1	62.5		3.6
1980–2005 (mm)	46.2	77.3	71.3	71.3 (LU1) 68.8 (LU2)	26.1
Change between two periods (mm)	−19.5	+9.2	+8.8	−2.5	+22.5
Contribution to the decrease of inflow to the reservoir		−47.2%	−45.1%	12.8%	115.4%

construction, and improvement in people's living conditions. As can be seen in Table 2, the direct water intake dramatically increased and precipitation slightly increased from period 1 to period 2, and thus, the direct impact of human activities could be considered as the main contributor to the decrease in inflow into the Panjiakou Reservoir. Direct impacts of human activities (direct water intakes) in the upper and lower catchments were 2.0 and 40.7 mm, respectively.

The indirect impact of human activities (land use/cover change) on annual runoff change was also assessed using the GBHM. Comparing LU2 to LU1, the area of forest was found to increase and the grassland decreased in the study area (see Table 1). The average NDVI values of LU1 and LU2 were 0.39 and 0.41, respectively, which mainly came from forest planting. Simulated mean annual inflow into the Panjiakou Reservoir during period 2 was 71.3 and 68.8 mm under the conditions of LU1 and LU2, respectively. Based on the simulation, the indirect impact of human activities on annual runoff change could be estimated to be about 2.5 mm, accounting for approximately 12.8% of the decrease in inflow into the Panjiakou Reservoir (see Table 4). The indirect impact of human activities on annual runoff change was a decrease of 1.3 and 3.1 mm for the upper and lower catchments, respectively.

DISCUSSION

Impacts of climate variability and human activities on runoff

Figure 6 shows the climate elasticity of runoff for the upper catchment (grassland dominated), the lower catchment (forest dominated), and the whole catchment (mixed vegetation). The values of ε_R^P were obtained as 1.5, 2.8, and 2.6 for the upper, lower, and whole catchments, respectively, indicating that a 1% increase in P could cause a 1.5%, 2.8% and 2.6% increase in R, respectively. Some previous studies showed similar results, for example, Ma *et al.* (2010) estimated $\varepsilon_R^P = 2.4$ in the Miyun catchment, belonging to the Hai River basin, using a two-parameter regression method. Yang & Yang (2011) calculated $\varepsilon_R^P = 2.6$ (range from 1.6 to 3.9) in the 89 catchments including the Hai River basin, using both a multiple regression method and a Budyko-based method. The precipitation elasticity of annual runoff ($\varepsilon_R^P = 2.8$) for the lower catchment was larger than that (1.5) for the upper catchment, which could be related to climate and soil conditions as reported by Dooge *et al.* (1999). The climate condition refers to humidity index, precipitation, stochastic nature of climate, and the soil condition refers to the field capacity of soils, soil moisture levels, length of soil water depletion, and saturated hydraulic conductivity. The antecedent precipitation elasticity of annual runoff ($\varepsilon_R^{P-1} = 0.8$) for the lower catchment was larger than that (0.3) for the upper catchment, possibly because the forest had strong rainfall infiltration that influenced the long-term baseflow in the river. The area ratio of forest and shrub in the lower catchment increased to 56.7% (see Table 1), whereas the grassland with relative shallow roots had difficulties in holding water in the upper catchment. The temperature elasticity of runoff (ε_R^T) was positive in the upper catchment but was negative in the lower catchment. The positive elasticity might be due to the snowmelt runoff in the upper catchment to a certain extent since it had higher elevation and colder climate, and the negative elasticity might have stronger evapotranspiration in the lower catchment due to the increase in air temperature.

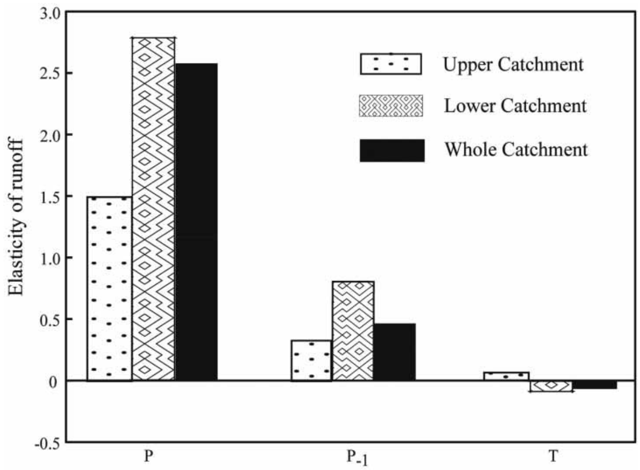

Figure 6 | The climate elasticity of annual runoff for the study catchment. (*Note: P* represents precipitation, P_{-1} represents antecedent precipitation, and *T* represents air temperature.)

Climate variability in this study primarily refers to the variation in precipitation and air temperature. Specifically, 28.5 mm of precipitation and 0.5 °C of air temperature increased from period 1 to period 2. Similar results are found in many reports; a declining trend in precipitation in most of the Hai River basin, but a rising trend in precipitation in the Luan River basin was detected during 1951 to 2000 (IPCC 2007; Xu *et al*. 2010).

The annual direct water intake of the whole catchment increased 22.5 mm from period 1 to period 2, a more dramatic increase than in the lower catchment. There is a greater population in the lower catchment than in the upper catchment. Therefore, with the increase in population, development of economic construction, and improvement in people's living conditions, the water demand for living, industry, and agriculture increased. Runoff could be strongly regulated by the soil with large water storage capacity due to the deep roots of trees in the forests. Comparing LU2 to LU1, the area of forest and shrub was found to increase and the grassland decreased in the study catchment (see Table 1). From Table 1, we can see that the area ratio of forest and shrub increased from 37.6 to 43.5% after the water–soil conservation project in the area in the 1980s, whereas the value of grassland decreased from 34.0 to 30.2%.

Uncertainty in the simulations

The current study used two different models, namely, the distributed hydrological model and climate elasticity model. The climate elasticity model is based on a regression method for estimating the impacts of climate variations on runoff. The GBHM, on the other hand, uses a physically based approach to simulate the impacts of climate variations on runoff. The two models were executed independently and were based on different time scales and their simulated results were compared with each other. The difference from runoff between the two periods simulated by the two models could then be used for comparison. Both the climate elasticity model and the GBHM obtained very similar results for the impact of climate variability on runoff (9.2 and 8.8 mm for the whole catchment simulated using the climate elasticity model and the GBHM, respectively) (see Table 4), which rendered great confidence on the impact assessment of this study.

The GBHM was used to evaluate the impacts of climate variability and human activities on runoff change. Major sources of uncertainty in the simulation from the GBHM may arise from the input data and model parameters. Precipitation data used as inputs to the models were obtained from 41 rainfall gauges and 10 meteorological gauges in and around the study catchment, which might be insufficient to cover a mountainous catchment area of 33,700 km^2. Although most model parameters were estimated based on the field data or land surface information, their uncertainties can also influence the simulation results. Validation of the GBHM shows that the RE of annual runoff was within 2.2%, which is much smaller than the magnitude of impacts of climate variability and human activities. However, simulation uncertainties should be further investigated in future studies.

The sum of all the contributions to the decrease in inflow into the Panjiakou Reservoir could be less than 100% because the contributors have cross impacts with one other. The climate variability could cause the changes in land-use features. Changes and variability in land use and land cover are major, but they are poorly recognized drivers of long-term global climate patterns (Pielke 2005). The changes in land use and land cover could also affect the climate. Pielke (2005) mentioned that the effects of spatially heterogeneous land use might at least be as important in altering the weather as changes in climate patterns associated with greenhouse gases. Kalnay & Cai (2003) found that half of the observed decrease in diurnal temperature range is due to urban and other land-use changes.

Land covers in the study catchment included the water body, urban area, forest, irrigated cropland, non-irrigated cropland, grassland, shrub, bare soil, and wetland. Finding a catchment with only one land cover type was difficult. The grassland- or forest-dominated catchments were simply used to distinguish the impacts of different vegetation types on runoff. Lack of NDVI data before 1980 might lead to an insufficient understanding of vegetation impact on runoff.

CONCLUSION

This study has analyzed the effects of climate variability and impacts of human activities on the decrease in runoff of the Panjiakou Reservoir catchment. A significant decrease of 0.91 mm/a was observed for annual runoff over the past 50 years, from 1956 to 2005. The annual precipitation non-significantly increased by 0.54 mm/a and the air temperature significantly increased by 0.023 °C/a. The study period was divided into two periods based on the sharp decrease of observed runoff and the dramatic increase of direct water intake from 1980. The impact of climate variability can be attributed to the significant temperature change, non-significant precipitation change, and other climatic factors. The direct impact of human activities can be attributed to the significant amount of direct water intake and indirect impact of human activities due to land use/cover change. The mean annual runoff of the whole catchment decreased by 19.5 mm from the sub-period 1956–1979 (65.7 mm) to the sub-period 1980–2005 (46.2 mm). Contributions to the decrease in runoff were quantified as follows:

1. The climate impact accounted for an increase in annual runoff by an estimated 9.2 and 8.8 mm for the Panjiakou Reservoir catchment using the GBHM and the climate elasticity model, respectively.
2. The annual direct water intake in the whole catchment increased by 22.5 mm, which was considered as the direct impact of human activities, accounting for 79.5% of the estimated decrease in annual runoff of the whole catchment.
3. The indirect impact of human activities through land use/cover change caused a decrease in annual runoff by an estimated 2.5 mm using the GBHM, accounting for about 8.8% of the decrease in annual runoff of the whole catchment.

Sub-catchments with different dominant vegetation types were also analyzed to distinguish differences in the runoff changes and their dominant drivers. The change in annual runoff contributed to the changes in the precipitation in the upper catchment (grassland dominated), lower catchment (forest dominated), and the whole catchment. The change in antecedent precipitation (a proxy of soil moisture) also contributed to the change in runoff in the lower catchment (forest dominated), implying stronger infiltration in the forest-dominated catchment. The temperature elasticity values were positive and negative for the upper and lower catchments, respectively, implying that the upper catchment had snowmelt runoff and the lower catchment had stronger evapotranspiration.

ACKNOWLEDGMENTS

The authors would like to thank the anonymous reviewers for their valuable comments and suggestions to improve the quality of the paper. The research was supported by the National Natural Science Foundation of China (Project No. 51025931, 50939004) and by the Ministry of Science and Technology of China (Grant No. 2011IM011000).

REFERENCES

Barnett, T. P., Pierce, D. W., Hidalgo, H. G., Bonfils, C., Santer, B. D., Das, T., Bala, G., Wood, A. W., Nozawa, T., Mirin, A. A., Cayan, D. R. & Dettinger, M. D. 2008 Human-induced changes in the hydrology of the western United States. *Science* **319**, 1080–1083.

Budyko, M. I. 1974 *Climate and life*. English edition edited by D. H. Miller. Academic Press, New York.

Burn, D. H. & Elnur, M. 2002 Detection of hydrologic trends and variability. *J. Hydrol.* **255**, 107–122.

Cong, Z., Yang, D., Gao, B., Yang, H. & Hu, H. 2009 Hydrological trend analysis in the Yellow River basin using a distributed hydrological model. *Water Resour. Res.* **45**, W00A13.

Costa, M. H. & Foley, J. A. 1997 Water balance of the Amazon Basin: dependence on vegetation cover and canopy conductance. *J. Geophys. Res.* **102**, 23973–23989.

Costa, M. H. & Foley, J. A. 1999 Trends in the hydrologic cycle of the Amazon basin. *J. Geophys. Res.* **104**, 14189–14198.

Déry, S. J. & Wood, E. F. 2005 Decreasing river discharge in northern Canada. *Geophys. Res. Lett.* **32**, L10401.

Dooge, J., Bruen, M. & Parmentier, B. 1999 A simple model for estimating the sensitivity of runoff to long-term changes in precipitation without a change in vegetation. *Adv. Water Resour.* **23**, 153–163.

Fu, B. P. 1981 On the calculation of the evaporation from land surface. *Sci. Atmos. Sin.* **5** (1), 23–31 (in Chinese).

Gerten, D., Rost, S., von Bloh, W. & Lucht, W. 2008 Causes of change in 20th century global river discharge. *Geophys. Res. Lett.* **35**, L20405.

IPCC 2007 *Climate Change 2007: The Physical Scientific Basis, Contribution of Working Group I to the Fourth Assessment Report of the Intergovernmental Panel on Climate Change*. Cambridge University Press, Cambridge, UK.

Kalnay, E. & Cai, M. 2003 Impact of urbanization and land-use change on climate. *Nature* **423**, 528–531.

Kendall, M. & Gibbons, J. D. 1990 *Rank Correlation Methods*. Oxford University Press, Oxford.

Li, L., Zhang, L., Wang, H., Wang, J., Yang, J., Jiang, D., Li, J. & Qin, D. 2007 Assessing the impact of climate variability and human activities on streamflow from the Wuding River basin in China. *Hydrol. Process*. **21**, 3485–3491.

Lins, H. F. & Slack, J. R. 1999 Streamflow trends in the United States. *Geophys. Res. Lett.* **26**, 227–230.

Ma, Z., Kang, S., Zhang, L., Tong, L. & Su, X. 2008 Analysis of impacts of climate variability and human activity on streamflow for a river basin in arid region of northwest China. *J. Hydrol.* **352**, 239–249.

Ma, H., Yang, D., Tan, S. K., Gao, B. & Hu, Q. 2010 Impact of climate variability and human activity on streamflow decrease in the Miyun Reservoir catchment. *J. Hydrol.* **389**, 317–324.

Maidment, D. R. 1992 *Handbook of Hydrology*. McGraw-Hill, New York.

Matheussen, B., Kirschbaum, R. L., Goodman, I. A., O'Donnell, G. M. & Lettenmaier, D. P. 2000 Effects of land cover change on streamflow in the interior Columbia River Basin (USA and Canada). *Hydrol. Process.* **14**, 867–885.

McCabe, G. J. & Wolock, D. M. 2002 A step increase in streamflow in the conterminous United States. *Geophys. Res. Lett.* **29** (24), 2185.

McClelland, J. W., Déry, S. J., Peterson, B. J., Holmes, R. M. & Wood, E. F. 2006 A pan-Arctic evaluation of changes in river discharge during the latter half of the 20th century. *Geophys. Res. Lett.* **33**, L06715.

Milliman, J. D., Farnsworth, K. L., Jones, P. D., Xu, K. H. & Smith, L. C. 2008 Climatic and anthropogenic factors affecting river discharge to the global ocean, 1951–2000. *Glob. Planet. Change* **62**, 187–194.

Nash, J. E. & Sutcliffe, J. V. 1970 River flow forecasting through conceptual models part I – a discussion of principles. *J. Hydrol.* **10** (3), 282–290.

NRC, N.C.R. 1991 *Opportunities in the Hydrologic Sciences*. National Academy Press, Washington, DC, USA.

Onstad, C. A. & Jamieson, D. G. 1970 Modeling the effect of land use modifications on runoff. *Water Resour. Res.* **6** (5), 1287–1295.

Piao, S., Friedlingstein, P., Ciais, P., de Noblet-Ducoudre, N., Labat, D. & Zaehle, S. 2007 Changes in climate and land use have a larger direct impact than rising CO_2 on global river runoff trends. *Proc. Natl. Acad. Sci. USA* **104**, 15242–15247.

Pielke, R. A. 2005 Land use and climate change. *Science* **310**, 1625–1626.

Qian, T., Dai, A. & Trenberth, K. E. 2007 Hydroclimatic trends in the Mississippi River basin from 1948 to 2004. *J. Clim.* **20**, 4599–4614.

Ren, X. S. 2007 *Water Resource Assessment in the Hai River Basin*. China Water Resources and Hydropower Press, Beijing.

Revelle, R. R. & Waggoner, P. E. 1983 Effects of a carbon dioxide-induced climate change on water supplies in the western United States. In: *Changing Climate*. Report of the Carbon Dioxide Assessment Committee, National Academy of Sciences, National Academy Press, Washington, DC.

Roderick, M. L. & Farquhar, G. D. 2011 A simple framework for relating variations in runoff to variations in climatic conditions and catchment properties. *Water Resour. Res.* **47**, W00G07.

Sankarasubramanian, A., Vogel, R. M. & Limbrunner, J. F. 2001 Climate elasticity of streamflow in the United States. *Water Resour. Res.* **37**, 1771–1781.

Scanlon, B. R., Jolly, I., Sophocleous, M. & Zhang, L. 2007 Global impacts of conversions from natural to agricultural ecosystems on water resources: quantity versus quality. *Water Resour. Res.* **43**, W03437.

Schaake, J. C. 1990 From climate to flow. In: *Climate Change and US Water Resources* (P. E. Waggoner, ed.). John Wiley, New York, pp. 77–206.

Tesemma, Z. K., Mohamed, Y. A. & Steenhuis, T. S. 2010 Trends in rainfall and runoff in the Blue Nile Basin: 1964–2003. *Hydrol. Process.* **24**, 3747–3758.

Twine, T. E., Kucharik, C. J. & Foley, J. A. 2004 Effects of land cover change on the energy and water balance of the Mississippi River basin. *J. Hydrometeorol.* **5**, 640–655.

Vogel, R. M., Wilson, I. & Daly, C. 1999 Regional regression models of annual streamflow for the United States. *J. Irrig. Drain. E-ASCE* **125**, 148–157.

Wang, J., Hong, Y., Gourley, J., Adhikari, P., Li, L. & Su, F. 2008 Quantitative assessment of climate change and human impacts on long-term hydrologic response: a case study in a sub-basin of the Yellow River, China. *Int. J. Climatol.* **30** (14), 2130–2137.

Xu, X. & Yang, D. 2009 *Analysing Inter-Annual Variability of the Water-Energy Balance in the Upstream Watershed of the Panjiakou Reservoir*. International Association of Hydrological Sciences, Wallingford, UK, pp. 87–96.

Xu, K., Milliman, J. D. & Xu, H. 2010 Temporal trend of precipitation and runoff in major Chinese Rivers since 1951. *Glob. Planet. Change* **73** (3–4), 219–232.

Xu, X., Yang, D. & Sivapalan, M. 2012 Assessing the impact of climate variability on catchment water balance and vegetation cover. *Hydrol. Earth Syst. Sci.* **16** (1), 43–58.

Xu, J., Yang, D., Yi, Y., Lei, Z., Chen, J. & Yang, W. 2008 Spatial and temporal variation of runoff in the Yangtze River basin during the past 40 years. *Quatern. Int.* **186**, 32–42.

Yang, D. & Musiake, K. 2003 A continental scale hydrological model using distributed approach and its application to Asia. *Hydrol. Process.* **17**, 2855–2869.

Yang, H. & Yang, D. 2011 Derivation of climate elasticity of runoff to assess the effects of climate change on annual runoff. *Water Resour. Res.* **47**, W07526.

Yang, D., Herath, S. & Musiake, K. 2002 A hillslope-based hydrological model using catchment area and width functions. *Hydrol. Sci. J.* **47**, 49–65.

Yang, D. W., Herath, S. & Musiake, K. 1998 Development of a geomorphology-based hydrological model for large catchments. *Annu. J. Hydraul. Eng. JSCE* **53**, 169–174.

Yang, D. W., Li, C., Hu, H. P., Lei, Z. D., Yang, S. X., Kusuda, T., Koike, T. & Musiake, K. 2004 Analysis of water resources variability in the Yellow River of China during the last half century using historical data. *Water Resour. Res.* **40**, W06502.

First received 17 October 2011; accepted in revised form 10 April 2013. Available online 9 May 2013